Numerical Simulations of Flat-walled Diffuser Elements for Valveless Micropumps

Anders Olsson*, Göran Stemme and Erik Stemme

Department of Signals, Sensors and Systems, Royal Institute of Technology, SE-100 44 Stockholm, Sweden
*Present address: IMC - Industrial Microelectronics Center, Electrum 233, SE-164 40 Kista
Tel: +46 8 752 10 00, Fax: +46 8 750 5430, E-mail: anders.olsson@imc.kth.se

ABSTRACT

The flow directing capability of micromachined flat-walled diffuser elements for valve-less micropumps have been investigated. The diffuser element is a small angle flow channel with a rounded inlet and a preferably sharp outlet. The diverging-wall direction is the positive flow direction. The commercial Computational Fluid Dynamics program ANSYS/Flotran (version 5.3) was used to simulate the flow pressure characteristic of several diffuser elements. The simulations are compared with experimental results. It is found that the simulated flow-pressure characteristic agrees well with the measured in the converging-wall direction and for Reynolds number below 300-400 in the diverging-wall direction. For higher Reynolds numbers the pressure loss in the diverging-wall direction is underestimated. The simulations are not sufficient for design optimization, but is very useful to increase the qualitative understanding of the flow in the diffuser element.

INTRODUCTION

During the last years, different types of valveless micropumps have been suggested [1-3]. They all use flow channels whose flow resistance is direction dependent. The idea to use such a channel in pumps was first mentioned in 1989 [4]. A finite element analysis of nozzles used as such channel was presented in 1990 [5]. The first working pump was the valveless diffuser pump presented in 1993 [1, 6, 7]. It uses channels with small opening angles around 10° as flow directing elements. The diverging wall direction is the positive flow direction. Measurements on fabricated valveless diffuser pumps indicate that the design of the diffuser elements is important for the performance [1, 6, 7].

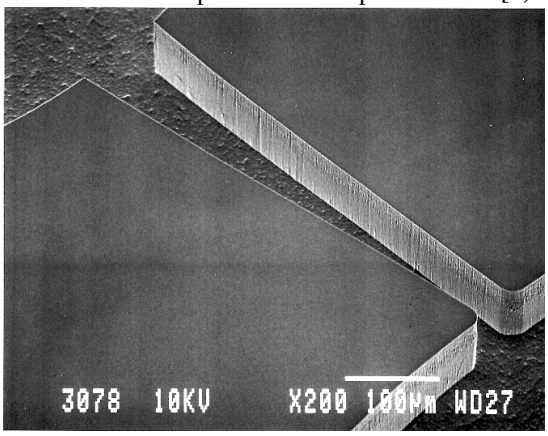

Figure 1. SEM-photo of an 80 µm deep diffuser element (DRIE by Alcatel CIT).

Although the geometry of the diffuser is simple, the flow is very complex [8]. The designer has to rely on experiments and simulations. For micromachined diffuser elements the available data is very limited [1, 9-11] and for flat-walled diffuser elements no data is available. There has been attempts made to do simplified analysis [10-12], but they are not sufficient for design optimization. To reduce the number of needed experiments to optimize the diffuser element design it would be useful if Computational Fluid Dynamics software could be used. A few attempts have been presented, [3, 13, 14], but no one of them is for micromachined flat-walled diffuser elements. This paper presents numerical simulations of micromachined flat-walled diffuser elements using the commercial CFD-program ANSYS/Flotran®.

FINITE ELEMENT MODEL

The finite element model was done for the type of micromachined diffuser elements used in previously reported micromachined flat-walled valveless diffuser pumps [7]. They were fabricated using deep reactive ion etching. A photo of such a diffuser element is shown in Figure 1. The diffuser element consists of a diffuser, a flow channel with expanding cross-section in the positive direction, with a rounded inlet and a preferably sharp outlet. A drawing is shown in Figure 2.

The simulations were done using a Dell PentiumPro 200 MHz. The used version of ANSYS/Multiphysics 5.3 allowed models with a maximum of 20,000 elements in Flotran. Simulations using both two- and three-dimensional models were done for several different diffuser elements with dimensions given in Table 1. In all case water was used as liquid, thereby limiting the problem to incompressible flow. The choice of laminar or turbulent flow is not obvious and both were tested. Normally a

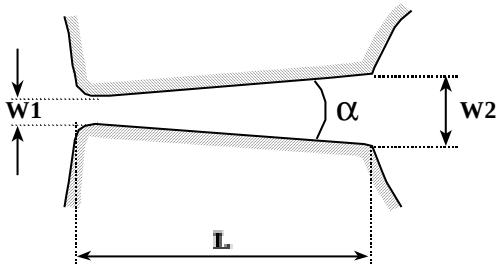

Figure 2. Top view of a flat-walled diffuser geometry where L is the diffuser length, α the divergence angle and W1 the neck width. The diffuser depth, B, is 80 µm. The inlet area $A_i=B\cdot W1$ and the outlet area $A_e=B\cdot W2$.

Table 1. Dimensions of diffuser elements together with measured pump performance [6] and diffuser element efficiency ratios. The notation is the same as used in [7].

	Notation	W1 [μm]	L [μm]	L/W1	α	Simulated 2D laminar η	Simulated 3D laminar η	Steady flow Measured η	Pump Performance Max. flow [μl/min]	Pump Performance Max. pressure [m H_2O]
Single Element	3a	80	1093	13.7	9.8°	2.08	1.18	1.45	1946	5.44
Pump Unit	3a	80	1093	13.7	9.8°	2.08	1.18	1.47	1946	5.44
Single Element	3b	80	1440	18.0	9.8°	2.24	1.48	1.51	1285	2.44
Single Element	3c	80	1093	13.7	7.0°	1.88	1.35	1.59	2270	7.57
Single Element	3d	80	1093	13.7	13°	3.20	1.75	1.32	2218	4.71

Reynolds number of 2300 is used as transitional number for macroscopic pipes with a sharp edge entrance and smooth walls [15]. This may be different for microfluidic components. For example, based on a formula given in [16] the transition number can be estimated to 400 for the actual diffuser dimensions. The transition to turbulence is also effected by the smoothness of the walls and the pressure gradient. Even a very small pressure increase usually brings transition with it [15]. The used software uses a two-equation turbulence model, usually called the k-ε turbulence model [17], to account for the turbulence.

RESULTS

The results from the simulations of the diffuser elements denoted 3a in Table 1 are shown in Figure 3. The simulations are compared with measured flow pressure characteristic. There is seen that for low Reynolds numbers the three-dimensional model agrees well with the experimental results. For higher Reynolds numbers, the two-dimensional model shows better agreement with the measurements. Especially there is good agreement between simulations and measurements in the nozzle direction. No significant difference is seen between the laminar and turbulent solutions. The effective viscosity calculated by the program indicates that the flow should be considered laminar. This is in agreement with the results of previous experimental studies [10, 11] of diffuser elements with other geometries. In the diffuser direction, the laminar solution gives the best result but here there is a significant difference between the measured and simulated values except for low Reynolds numbers. No significant difference is seen between the laminar and turbulent flow models. For low Reynolds numbers, the three-dimensional model gives best result and for high Reynolds numbers, the two-dimensional model gives best result. For the two-dimensional model with laminar flow the point at $Re \approx 1100$ sticks out and actually is on the measured curve. A study of the flow pattern shows gross flow separation. Probably there are numerical problems and the concurrence with the experiment is probably just a coincidence.

The laminar and turbulent simulations did not differ significantly and for the diffuser elements with other geometrical dimensions, simulations were only done using laminar flow. The simulations were done for the pressure range 0-100 kPa using two-dimensional models and for Reynolds numbers below 400 using three-dimensional models. The results are presented in Table 1. In the table, results from steady flow measurements are presented as the diffuser element efficiency ratio, η. It is defined as

$$\eta = \frac{\xi_{negative}}{\xi_{positive}} \tag{1}$$

where $\xi_{negative}$ is the pressure loss coefficient in the negative flow direction and $\xi_{positive}$ that in the positive flow direction.

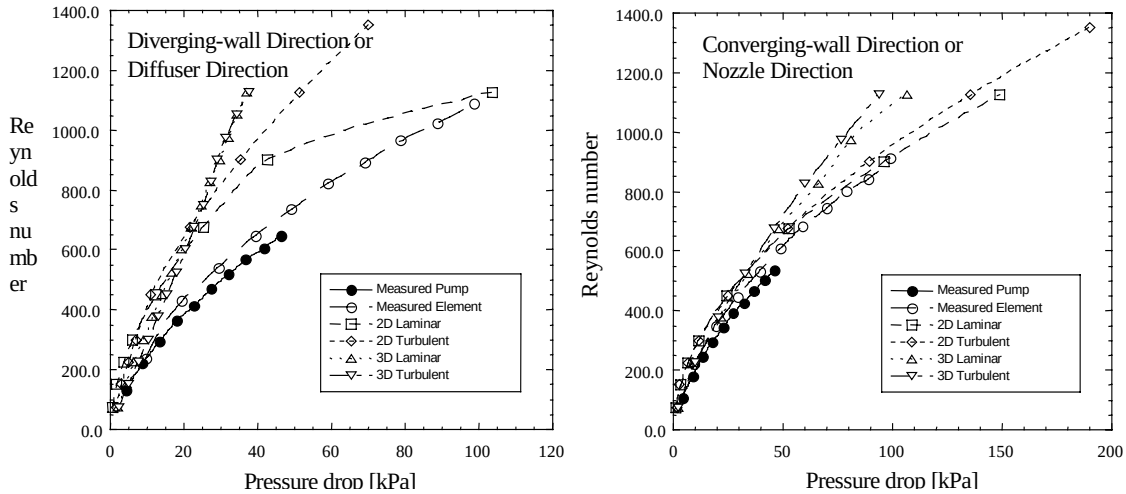

Figure 3. Measured and simulated flow-pressure characteristic for the diffuser element denoted 3a in Table 1

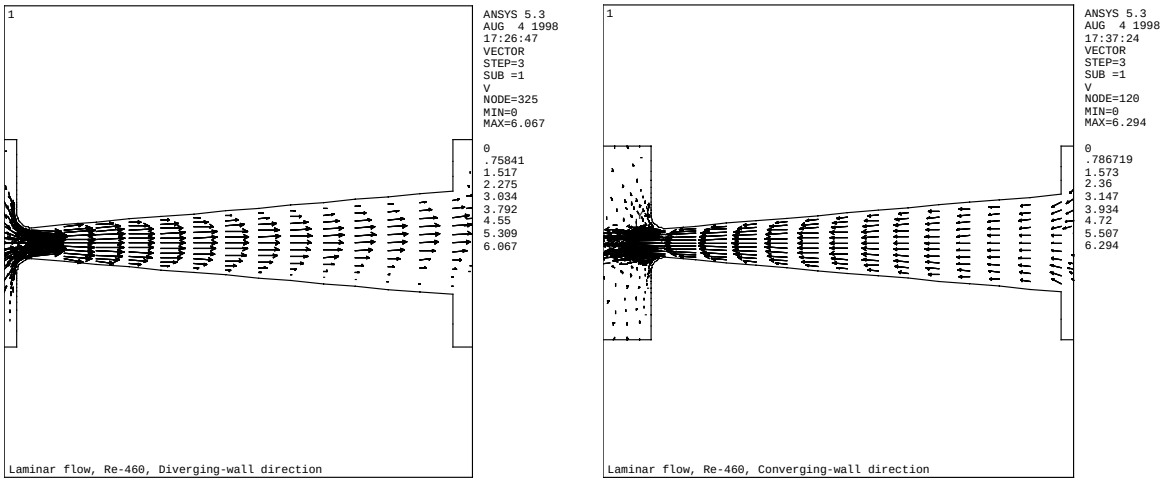

Figure 4. Flow patterns simulated for a 2-dimensional model of a diffuser element of length 1.093 mm, opening angle 9.8° and smallest width 80µm. The laminar flow model was used and the number of elements is fewer than normally used to make the arrows clearer. The Reynolds number is 460.

The pressure loss coefficient, ξ, comes from the formula normally used to relate the pressure drop, Δp, and the mean flow velocity in the throat, $\overline{u}_{throat}$, of a diffuser or nozzle:

$$\Delta p = \xi \cdot \frac{1}{2} \rho \overline{u}_{throat}^2 \qquad (2)$$

where ρ is the fluid density. For good pump performance η should be as high as possible.

Figure 4 shows typical simulated flow pattern for a diffuser element. In the positive diverging-wall direction it is seen that the velocity is reduced before the exit and the remaining kinetic energy is then lost in a jet at the outlet. In the opposite converging-wall direction the flow accelerates through the nozzle to high velocity. The kinetic energy is lost in a jet at the outlet. In the diverging-wall direction the laminar solution shows a small asymmetry at the outlet that not is seen for the turbulent solution.

Simulations were also done for sharp edged element with a large opening angle. The length was 1.093 mm, the opening angle 70° and the smallest width 80 µm. Typical flow patterns are shown in Figure 5. Only the upper half of the element is modeled and center axis is used as symmetry axis. The reason is that the full model gave a strong asymmetric flow pattern where the main flow stream follows along one of the walls. It is not clear if this effect is due to an unsteady flow situation or due to the used numerical solver. The qualitative result is the same for the both full and the half model and in the diverging-wall direction there is gross flow separation. The effective cross-sectional area is smaller than the actual opening. This is a vena-contracta effect probably caused by the sharp inlet. In the converging-wall direction the vena-contracta effect is much smaller. This explains the seen direction dependent flow resistance with the converging-wall direction as positive flow direction. Figure 6 shows the pressure distribution along the center axis for the same flow situation.

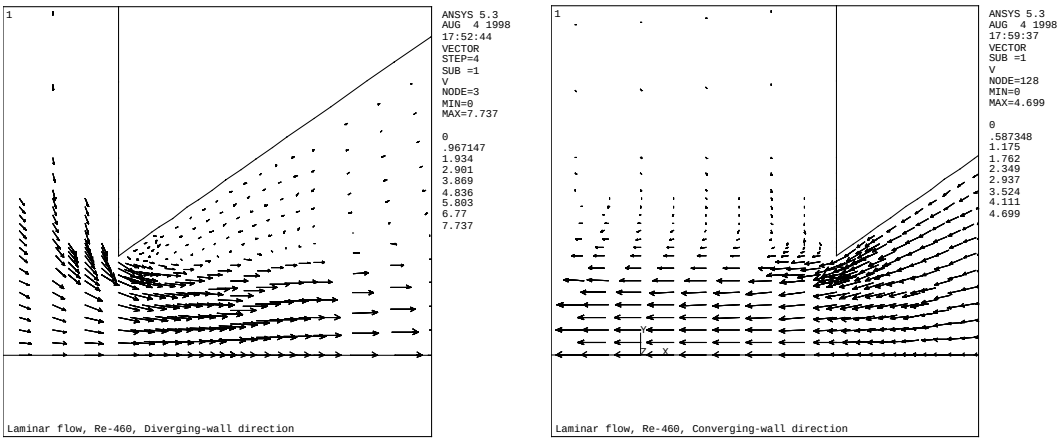

Figure 5. Flow patterns simulated for a 2-dimensional model of a nozzle element of length 1.039 mm, opening angle 70° and smallest width 80 µm. The laminar flow model was used and the number of elements is fewer than normally used to make the arrows clearer. The Reynolds number is 460.

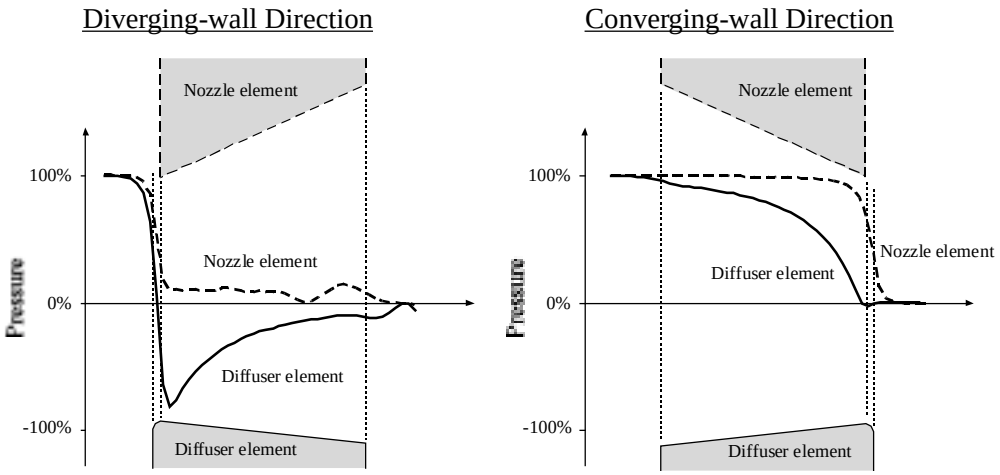

Figure 6. Pressure distribution along the symmetry axis for the same load cases as in Figure 4 and Figure 5 but using the full finite element models.

CONCLUSION

Micromachined flat-walled diffuser elements have been investigated. Numerical simulations have been done using the commercial CFD program ANSYS/Flotran. The simulations have been compared with experimental results.

The simulations show the flow directing effect of the diffuser elements. For low Reynolds numbers the simulations predicted the flow-pressure characteristic well. Three-dimensional models gave better results than two-dimensional models. For high Reynolds numbers the simulations predict the flow-pressure characteristic well in the converging-wall direction, but in the diverging-wall direction the difference between simulations and measurements are significant. The two-dimensional models gave better result than the three dimensional model. This is probably due to the finer mesh possible to use in the two-dimensional model. No significant difference was seen in the flow-pressure characteristics between turbulent and laminar simulations, but for Reynolds numbers above approximately 400 a turbulent flow situation could possibly be expected. The reason that no difference is seen may be that the turbulence models available in the used software is not sufficient to describe turbulent flow for actual Reynolds numbers and for a diverging flow-channel [18,19]. The results achieved with the used software are today not accurate enough to be used for design optimization of valve-less diffuser micropumps. The simulations are however very useful to increase the qualitative understanding of the diffuser element flow.

The investigation has also shown that diffuser element with small opening angles and nozzle elements with large opening angles is based on different effects. In the diffuser element there is strong pressure recovery in the diffuser in the diverging-wall direction (see Figure 6) and flow separation is probably small. In the nozzle element the opening angle is so large that there is gross flow separation and no pressure recovery. Instead, the nozzle element relies on ”vena-contracta” effects in both directions. The losses are actually higher than in the converging-wall direction and the positive flow direction is opposite to that of the diffuser element.

ACKNOWLEDGMENT

This work was supported by the Swedish National Board for Industrial and Technical Development (NUTEK).

REFERENCES

[1] Stemme et al, Sensors and Actuators. A, 39 (1993) 159-67.
[2] Gerlach et al, J. Micromech. Microeng., 5 (1995) 199-201.
[3] Forster et al, “Design, fabrication and testing of fixed-valve micro-pumps,” Proceedings of the ASME Fluids Engineering Division ASME 1995, FED-Vol. 234, 1995 IMECE, 1995, pp. 39-44.
[4] F. C. M. van de Pol, Thesis: A pump based on micro-engineering techniques, University of Twente, Enschede, the Netherlands, 1989
[5] Smith, “Micromachined nozzles fabricated with replicative method,” Micromechanics Europe 1990 (MME '90), Berlin, Germany, 26-27 November, 1990, pp. 53-57.
[6] Olsson et al, J. Microelectromech. Syst., 6 (1997) 161-66.
[7] Olsson et al, J. Micromech. Microeng., 6 (1996) 87-91.
[8] Tsui et al, ASME J. Fluids Eng., 117 (1995) 612-16.
[9] Olsson et al, Sensors and Actuators A, 46-47 (1995) 549-56.
[10] Olsson et al, Sensors and Actuators A, 57 (1996) 137-43.
[11] Heschel et al, J. Microelectromech. Syst., 6 (1997) 41-47.
[12] Gerlach, Sensors and Actuators A, 69 (1998) 181-91.
[13] Koch et al, J. Micromech. Microeng., 8 (1998) 119-22.
[14] Olsson et al, “Simulation Studies of Diffuser and Nozzle Elements for Valve-less Micropumps,” Transducers 97, Chicago, USA, June 15-19, 1997, pp. 1039-1042.
[15] H. Schlichting, Boundary-layer theory, 7th ed. New-York: McGraw-Hill, Inc., 1979.
[16] Gravesen et al, J. Micromech. Microeng., 3 (1993) 168-82.
[17] ANSYS CFD FLOTRAN Analysis Guide Release 5.3, 1 ed. Houston, Pennsylvania: ANSYS, Inc., 1996.
[18] Lai et al, AIAA-Journal, 27 (1989) 542-8
[19] Nagano et al, J. Fluids Eng., 109 (1987) 156-60.